Modeling and Control of Robot-Structure Coupling During In-Space Structure Assembly

Sean Swei, Benjamin Jenett, Nick Cramer, Kenneth Cheung

Intelligent Systems Division, NASA Ames Research Center, Moffett Field, California 94035, USA

This paper considers the problem of robot-structure coupling dynamics during in-space robotic assembly of large flexible structures. A two-legged walking robot is used as a construction agent, whose primary goal is to stably walking on the flexible structure while carrying a substructure component to a designated location. The reaction forces inserted by the structure to the walking robot are treated as bounded disturbance inputs, and a trajectory tracking robotic controller is proposed that combines the standard full state feedback motion controller and an adaptive controller to account for the disturbance inputs. In this study, a reduced-order Euler-Bernoulli beam structure model is adapted, and a finite number of co-located sensors and actuators are distributed along the span of the beam structure. The robot-structure coupling forces are treated as a bounded external forcing function to the structure, and hence an output covariance constraint problem can be formulated, in terms of linear matrix inequality, for optimal structure control by utilizing the direct output feedback controllers. The numerical simulations show the effectiveness of the proposed robot-structure modeling and control methodology.

I.   Introduction

The expansion of future human space exploration to Moon, Mars and beyond requires creation of ultra-large and flexible structures that would provide basic operational and functional needs in space. For instance, many proposed space missions envision utilization of large space structures, such as communication antennas, astronomical observatories, and solar power stations, to just name a few. One class of materials that has recently been considered for such application is the digital composite metamaterials. These are made of a large number of physical components, but with a small number of distinctive part types.[1] Because of this high repetitive patterns in size/dimension and shape, the autonomous or robotic in-space structure assembly becomes a tractable and viable solution for building large space structures. While Jenett et al.[2] investigated materials/structures and robotic related technical challenges in assembling kilometer-scale space structures, this paper focuses on modeling of coupling dynamics between walking robots and vibrating flexible structures during in-space robotic assembly, and controlling/suppressing excessive structure vibration by utilizing advanced control techniques.

Large flexible space structures exhibit some distinctive characteristics,[3] which include: 1) low resonant frequencies; often densely clustered; 2) very low natural damping; 3) very stringent mission requirements on, for instance, pointing accuracy and alignment/orientation. Therefore, as a result of the presence of lightly damped low-frequency structure modes, when a large space structure is disturbed or excited, it is likely to remain in vibration for quite some time, if no counter measurement, such as active/passive structural control, is implemented. Furthermore, the robot-structure coupling dynamics imposes a unique challenge for in-space robotic assembly, because a walking robot can be a source of structural vibration through robot-structure interaction and will degrade the performance of structure build-up. Therefore, it is imperative to develop a dynamic model that could accurately depict the robot-structure coupling effect and provide a mathematical framework for formulating externally/internally actuated active/passive mechanisms for suppression of structural vibration.

Modeling of large flexible and spatially periodic structures by utilizing distributed parameter approach often results in a large dimensional system description. As a consequence, the resultant model does not fit to be used for practical control design, since the limited control authority and actuator bandwidth will inevitably impose additional constraints on achievable overall structure performance. Therefore, in order to effectively assess the structure performance, in this paper a reduced-order control-centric robot-structure coupling dynamic model is developed, and subsequently used for designing optimal structural controllers.

In contrast to the conventional control of structure approach, the proposed in-space robotic assembly framework allows potential use of both walking robots and (some) instrumented building-block structure components to be ac-

American Institute of Aeronautics and Astronautics

tive/passive actuation agents, so as to achieve improved structure performance while maintaining robotic efficiency. The challenges of this cooperative actuation include: 1) workload break down between the two active agents; 2) simplicity of actuation mechanisms; and 3) synchronous and collaborative execution of two agents. In this paper, a mechanically compact and multi-functional two degree-of-freedom walking robot, known as BiLL-E, developed in Jenett and Cheung[4] is adapted and used for building up the space structures, as illustrated in Fig. 1. This robot-structure teaming in the control of space structure is novel, in which the walking robots can be considered as actuators that are "re-configurable" depending on the mission needs. In addition, the needed sensor suite can also be instrumented as part of robot hardware, enabling also "re-configurable" sensors, which are naturally co-located with actuators and in compatible units, e.g. angular rate vs. torque and acceleration vs. force. The objective of this paper is to develop a theoretical framework for modeling and control of a coupled robot-structure problem, so that a numerically tractable problem formulation can be derived and solved.

This paper is organized as follows. Section II presents the two-legged robot (BiLL-E) and its equations of motion, which includes the reaction forces from the coupled structure. The Euler-Bernoulli beam structure model is presented in Section III and the structure dynamics is derived by enforcing the "free-free" boundary conditions. Section IV contains the development of robotic and adaptive controller for trajectory tracking. Section V presents the output covariance constraint problem for optimal structure control by utilizing a static output feedback controller, and the numerical simulations are presented in Section VI. Finally, some concluding summaries and future research are contained in Section VII.

Courtesy of Benjamin Jenett, ARC

Figure 1. A robot (Bill-E) assembling lattice structures

II. Walking Robot on a Structure

The robot-structure coupled system (RSCS) is graphically depicted in Fig 2, where M_i, I_i, L_i, θ_i, and τ_i are mass, moment of inertia, length, inclination angle, and applied torque at ith leg, $i = 1, 2$. In addition, in Fig. 3 $w(x,t)$ denotes the transverse deflection of flexible structure. To derive the equations of motion for RSCS, we first utilize the Lagrange equations as follows,

$$\frac{d}{dt}\left(\frac{\partial L}{\partial \dot{q}}\right) - \frac{\partial L}{\partial q} = Q, \tag{1}$$

where $L = T - V$ is a Lagrangian where T denotes the total kinetic energy and V the total potential energy, and Q is a vector of generalized forces (or moments) acting in the direction of generalized coordinates q. In referring to Figs. 2 and 3, the total kinetic and potential energies of RSCS can be written as sum of energies of individual components, and they are given by

$$
\begin{aligned}
T_1 &= \tfrac{1}{2}M_1[(l_1\dot{\theta}_1\cos\theta_1 - \dot{w})^2 + (l_1\dot{\theta}_1\sin\theta_1)^2] + \tfrac{1}{2}I_1\dot{\theta}_1^2, \\
T_2 &= \tfrac{1}{2}M_2[(l_2\dot{\theta}_2\cos\theta_2 - L_1\dot{\theta}_1\sin\theta_1)^2 + (L_1\dot{\theta}_1\cos\theta_1 + l_2\dot{\theta}_2\sin\theta_2 - \dot{w})^2] + \tfrac{1}{2}I_2\dot{\theta}_2^2, \\
V_1 &= M_1 g l_1 \sin\theta_1 - M_1 g w, \\
V_2 &= M_2 g(L_1\sin\theta_1 - l_2\cos\theta_2) - M_2 g w,
\end{aligned}
$$

where T_i and V_i; $i = 1,2$, denote the kinetic and potential energies of ith leg, and $l_i = L_i/2$. Moreover, the generalized force/moment vector $Q = [\tau_1, \ \tau_2, \ -f_z]$, where f_z is the reaction force at the foot of leg-1; see Fig. 3. Though the space structure is the primary subject of consideration in this paper, however, in derivation we decided to retain the gravity terms, so that we could perform model validation through experiments in 1-g environment, if needed. These gravity

American Institute of Aeronautics and Astronautics

terms can be readily removed for 0-g simulations. Substituting the above equations into (1) yields the equations of motion for a walking robot as follows,

$$(M_1 l_1^2 + M_2 L_1^2 + I_1)\ddot{\theta}_1 + M_2 l_2 L_1 \ddot{\theta}_2 \sin(\theta_2 - \theta_1) + M_2 l_2 L_1 \dot{\theta}_2^2 \cos(\theta_2 - \theta_1)$$
$$+ (M_1 l_1 + M_2 L_1)(g - \ddot{w}) \cos\theta_1 = \tau_1,$$
(2a)

$$(M_2 l_2^2 + I_2)\ddot{\theta}_2 + M_2 l_2 L_1 \ddot{\theta}_1 \sin(\theta_2 - \theta_1) - M_2 l_2 L_1 \dot{\theta}_1^2 \cos(\theta_2 - \theta_1)$$
$$+ M_2 l_2 (g - \ddot{w}) \sin\theta_2 = \tau_2,$$
(2b)

$$(M_1 + M_2)\ddot{w} - (M_1 l_1 + M_2 L_1)\ddot{\theta}_1 \cos\theta_1 + (M_1 l_1 + M_2 L_1)\dot{\theta}_1^2 \sin\theta_1$$
$$- M_2 l_2 (\ddot{\theta}_2 \sin\theta_2 + \dot{\theta}_2^2 \cos\theta_2) - (M_1 + M_2)g = -f_z.$$
(2c)

Note that the equations of motion obtained above are highly coupled and nonlinear, where $(\theta_1, \theta_2, \dot{\theta}_1, \dot{\theta}_2, w, \dot{w})$ denote the states and (τ_1, τ_2) the robot control inputs. The robot-structure coupling force f_z is unknown, hence we will need one more equation, which can be supplemented by structure dynamics in the next section.
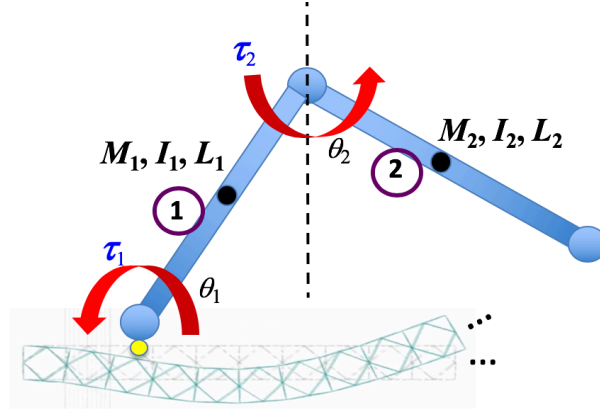

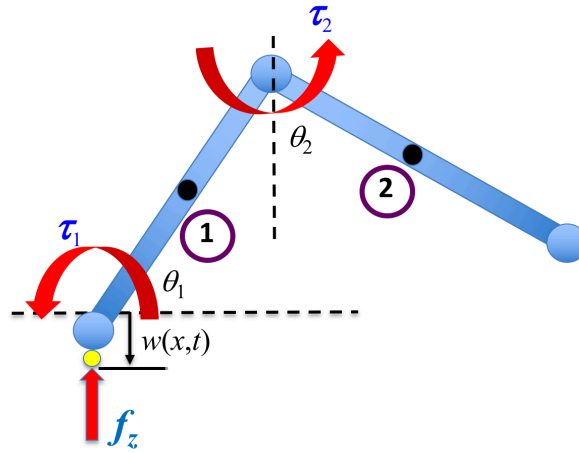Figure 2. Schematics of a walking robot on flexible structure

Figure 3. Free-body diagram showing coupling force between robot and structure

III. Euler-Bernoulli Beam

In this paper, we assume the space structure can be formulated as an Euler-Bernoulli (EB) beam, hence for the varying contact force problem shown in Fig. 3, after utilizing Euler-Lagrange equation, the equations of motion for EB beam subject to an external force applied at $x = x_v$ can be described by

$$EI\frac{\partial^4 w(x,t)}{\partial x^4} + \rho A \frac{\partial^2 w(x,t)}{\partial t^2} = f_z(\theta_1, \theta_2)\,\delta(x - x_v),$$
(3)

American Institute of Aeronautics and Astronautics

where E is the young's modulus, I the moment of inertia, ρ the density, and A the cross-section area. In addition, $f_z \delta(x - x_v)$ denotes the contact force at x_v and δ the Dirac function. We assume that both EI and ρA are constants. By utilizing Ritz-Galerkin's method, the transverse deflection of EB beam $w(x,t)$ can be approximated by

$$w(x,t) \approx \sum_{i=1}^{n} v_i(t) \cdot \Phi_i(x), \tag{4}$$

where $\Phi_i(x)$ denotes the ith normalized eigenfunction (or mode shape), $v_i(t)$ the corresponding generalized coordinate (for deflection), and n the number of retained modes. Note that for a "free-free" beam structure of length L, the mode shape $\Phi_i(x)$ is given by

$$\Phi_i(x) = \sin(\mu_i x) + \sinh(\mu_i x) + \frac{\cos(\mu_i L) - \cosh(\mu_i L)}{\sin(\mu_i L) + \sinh(\mu_i L)} [\cos(\mu_i x) + \cosh(\mu_i x)], \ i = 1, 2, \cdots, n, \tag{5}$$

where $\mu_i L$ are solutions to the following eigenvalue problem,

$$\cos(\mu L) \cdot \cosh(\mu L) = 1 \,.$$

Now, substituting (4) into (3) renders,

$$EI \sum_{i=1}^{n} v_i(t) \frac{d^4 \Phi_i(x)}{dx^4} + \rho A \sum_{i=1}^{n} \ddot{v}_i(t) \Phi_i(x) = f_z(\theta_1, \theta_2) \delta(x - x_v) \,. \tag{6}$$

III.A. A weak-form representation

The "weak-form" integral representation of the free-free beam dynamic equations can be attained by pre-multiplying (6) by $\Phi_j(x)$ and integrating over the beam length L, and we obtain

$$EI \sum_{i=1}^{n} v_i(t) \int_0^L \Phi_j(x) \frac{d^4 \Phi_i(x)}{dx^4} dx + \rho A \sum_{i=1}^{n} \ddot{v}_i(t) \int_0^L \Phi_j(x) \Phi_i(x) dx = \int_0^L \Phi_j(x) f_z(\theta_1, \theta_2) \delta(x - x_v) dx \,. \tag{7}$$

Note that by applying the integration by parts to the first integral term yields

$$\int_0^L \Phi_j(x) \frac{d^4 \Phi_i(x)}{dx^4} dx = (\Phi_j(x) \frac{d^3 \Phi_i(x)}{dx^3})_0^L - (\frac{d\Phi_i(x)}{dx} \frac{d^2 \Phi_i(x)}{dx^2})_0^L + \int_0^L \frac{d^2 \Phi_j(x)}{dx^2} \frac{d^2 \Phi_i(x)}{dx^2} dx \,,$$

hence, by enforcing that the forces and moments vanish at the boundaries for a free-free beam, we obtain

$$\int_0^L \Phi_j(x) \frac{d^4 \Phi_i(x)}{dx^4} dx = \int_0^L \frac{d^2 \Phi_j(x)}{dx^2} \frac{d^2 \Phi_i(x)}{dx^2} dx \,.$$

Therefore, Eq. (7) can be rewritten as

$$\sum_{j=1}^{n} [m_{i,j} \ddot{v}_j(t) + k_{i,j} v_j(t)] = F_i \,, \ i = 1, 2, \cdots, n, \tag{8}$$

where

$$m_{i,j} = \rho A \int_0^L \Phi_i(x) \Phi_j(x) dx \,, \ k_{i,j} = EI \int_0^L \frac{d^2 \Phi_j(x)}{dx^2} \frac{d^2 \Phi_i(x)}{dx^2} dx \,,$$

$$F_i = \int_0^L \Phi_i(x) f_z(\theta_1, \theta_2) \delta(x - x_v) dx = \Phi_i(x_v) f_z(\theta_1, \theta_2) \,.$$

Furthermore, (8) can be equivalently described in a matrix form as

$$M_s \ddot{p}(t) + K_s p(t) = B(x_v) f_z(\theta_1, \theta_2) \,, \tag{9}$$

where $p(t) = [v_1(t), v_2(t), \cdots, v_n(t)]^T$ and

$$M_s = \begin{bmatrix} m_{1,1} & m_{1,2} & \cdots & m_{1,n} \\ m_{1,2} & m_{2,2} & \cdots & m_{2,n} \\ \vdots & \vdots & \cdots & \vdots \\ m_{1,n} & m_{2,n} & \cdots & m_{n,n} \end{bmatrix}, \ K_s = \begin{bmatrix} k_{1,1} & k_{1,2} & \cdots & k_{1,n} \\ k_{1,2} & k_{2,2} & \cdots & k_{2,n} \\ \vdots & \vdots & \cdots & \vdots \\ k_{1,n} & k_{2,n} & \cdots & k_{n,n} \end{bmatrix}, \ B(x_v) = \begin{bmatrix} \Phi_1(x_v) \\ \Phi_2(x_v) \\ \vdots \\ \Phi_n(x_v) \end{bmatrix}.$$

Note that M_s and K_s denote the structure mass and stiffness property, and they are symmetric (and positive-definite) matrices. Any flexible structure possesses some level of damping effect, hence an estimated damping term $C_s \dot{p}(t)$ is injected into (9), where the damping matrix C_s is derived in the next section.

III.B.   Derivation of damping matrix

Given the structure mass and stiffness matrices M_s and K_s, we first perform singular value decomposition for M_s to obtain

$$M_s = U_1 \Lambda_1 U_1^T,$$

where U_1 is an orthonormal matrix, i.e. $U_1^T U_1 = I$, and Λ_1 a diagonal matrix. Let T_1 be defined as

$$T_1 = U_1 \Lambda_1^{\frac{1}{2}},$$

and perform singular value decomposition for $T_1^T K_s T_1$, that is

$$T_1^T K_s T_1 = U_2 \Lambda_2 U_2^T,$$

where $U_2^T U_2 = I$ and $\Lambda_2 = \mathrm{diag}\left\{\omega_1^2, \omega_2^2, \dots\right\}$; ω_i denotes the ith undamped natural frequency. Let $T_2 = U_2$ and $T = T_1 T_2$, then the damping matrix C_s can be given by

$$C_s = 2T^{-T} \mathscr{Z} \Omega T^{-1}, \tag{10}$$

where $\mathscr{Z} = \mathrm{diag}\left\{\zeta_1, \zeta_2, \dots\right\}$; ζ_i denotes the (estimated) ith structure mode damping ratio, and $\Omega = \mathrm{diag}\left\{\omega_1, \omega_2, \dots\right\}$. In practice, the structure damping ratios can be estimated through a series of bench tests. Finally, with augmented damping term, (9) can now be rewritten as

$$M_s \ddot{p}(t) + C_s \dot{p}(t) + K_s p(t) = B(x_v) f_z(\theta_1, \theta_2). \tag{11}$$

IV.   Robotic Controller Design

Note that the transverse deflection of EB beam $w(x,t)$ given in (4) can be expressed in a compact form as

$$w(x,t) \approx \sum_{i=1}^{n} v_i(t) \cdot \Phi_i(x) = B^T(x) p(t),$$

similarly $\ddot{w}(x,t)$ can be given by

$$\ddot{w}(x,t) \approx B^T(x) \ddot{p}(t). \tag{12}$$

Now, substituting (12) into (2) gives the coupled robot-structure dynamic equations as

$$(M_1 l_1^2 + M_2 L_1^2 + I_1)\ddot{\theta}_1 + M_2 l_2 L_1 \ddot{\theta}_2 \sin(\theta_2 - \theta_1) + M_2 l_2 L_1 \dot{\theta}_2^2 \cos(\theta_2 - \theta_1) - (M_1 l_1 + M_2 L_1) B^T \ddot{p} \cos\theta_1 = \tau_1, \tag{13a}$$
$$(M_2 l_2^2 + I_2)\ddot{\theta}_2 + M_2 l_2 L_1 \ddot{\theta}_1 \sin(\theta_2 - \theta_1) - M_2 l_2 L_1 \dot{\theta}_1^2 \cos(\theta_2 - \theta_1) - M_2 l_2 B^T \ddot{p} \sin\theta_2 = \tau_2, \tag{13b}$$

where the gravity terms are omitted to simulate a space environment. The coupled equations of motion presented above describe the robot-structure interaction of a walking robot with either leg-1 or leg-2 moving forward. Equivalently, Eq. (13) can be expressed in a compact form as

$$D(q)\ddot{q} + C(q,\dot{q})\dot{q} - H(q)\ddot{p} = \tau, \tag{14}$$

where $q = [\theta_1\ \theta_2]^T$, $\tau = [\tau_1\ \tau_2]^T$, and

$$D(q) = \begin{bmatrix} M_1 l_1^2 + M_2 L_1^2 + I_1 & M_2 l_2 L_1 \sin(\theta_2 - \theta_1) \\ M_2 l_2 L_1 \sin(\theta_2 - \theta_1) & M_2 l_2^2 + I_2 \end{bmatrix}, H(q) = \begin{bmatrix} (M_1 l_1 + M_2 L_1)\cos\theta_1 B^T \\ M_2 l_2 \sin\theta_2 B^T \end{bmatrix},$$
$$C(q,\dot{q}) = \begin{bmatrix} 0 & M_2 l_2 L_1 \dot{\theta}_2 \cos(\theta_2 - \theta_1) \\ -M_2 l_2 L_1 \dot{\theta}_1 \cos(\theta_2 - \theta_1) & 0 \end{bmatrix}.$$

It should be noted that the matrices $D(q)$ and $C(q,\dot{q})$ satisfy the following properties.

Property I: $D(q)$ is a positive definite symmetric matrix for all q.

Property II: $\dot{D}(q) - 2C(q,\dot{q})$ is a skew-symmetric matrix for all q and $\dot{q} \neq 0$.

These properties are commonly being used when deriving for stabilizing robotic controllers.[5]

IV.A.   Adaptive trajectory tracking

Let $q_d(t)$ be a desired trajectory and $e = q(t) - q_d(t)$ the error. Then, $\dot{e}(t) = \dot{q}(t) - \dot{q}_d(t)$ and $\ddot{e}(t) = \ddot{q}(t) - \ddot{q}_d(t)$. In addition, we assume that both $q(t)$ and $\dot{q}(t)$ are measurable.

Note that Eq. (14) describes a standard robot dynamics, but subjected to structure coupling dynamics. Therefore, we propose that the robot controller $\tau(t)$ be consisted of two parts; namely,

$$\tau(t) = u_{sf}(t) + u_a(t),$$

where u_{sf} denotes the standard trajectory tracking state-feedback controller for stand-alone robot, while u_a is the adaptive controller to account for the structure coupling effect $H(q)\ddot{p}$. Furthermore, we may treat this coupling effect as a disturbance input to the walking robot. Hence, let the disturbance input $g(t) = H(q)\ddot{p}$ be represented by

$$g(t) = \bar{\Theta}^T \Pi(t), \tag{15}$$

where $\bar{\Theta}$ is an unknown constant matrix and $\Pi(t)$ a known vector of basis functions, such as Chebyshev polynomials. Now, the proposed control law is given by

$$\tau(t) = \underbrace{-k_p e(t) - k_d \dot{e}(t) + D(q)\ddot{q}_d + C(q,\dot{q})\dot{q}_d}_{u_{sf}} - \underbrace{\Theta^T(t)\Pi(t)}_{u_a}, \tag{16}$$

where $k_p > 0$ and $k_d > 0$ are the attitude and rate control gain matrices, respectively, and $\Theta(t)$ the adaptive parameter that estimates $\bar{\Theta}$. To this end, we should emphasize that our ultimate control design goal is to ensure asymptotic trajectory tracking, i.e. $e(t) \to 0$ as $t \to \infty$. In other words, whether $\Theta(t) \to \bar{\Theta}$ as $t \to \infty$ is not our primary design objective, as long as $\Theta(t)$ is bounded.

Now, substituting (16) and (15) into (14), and after simple algebraic manipulations, yields the feedback-controlled system described by

$$D(q)\ddot{e} + C(q,\dot{q})\dot{e} = -k_p e - k_d \dot{e} + \tilde{\Theta}^T(t)\Pi(t), \tag{17}$$

where $\tilde{\Theta}(t) = \bar{\Theta} - \Theta(t)$ denotes the estimation error. Next, we propose the following adaptation law for $\tilde{\Theta}(t)$ or $\Theta(t)$,

$$\dot{\tilde{\Theta}}(t) = \dot{\Theta}(t) = -\Gamma \Pi(t)\dot{e}^T(t), \tag{18}$$

where $\Gamma > 0$ is a constant adaptive gain matrix. In what follows, we shall prove that (17) with the adaption law given in (18) ensures the asymptotic trajectory tracking for a walking robot.

IV.B.   A Lyapunov approach

Let $V(e,\dot{e},\tilde{\Theta}) = \frac{1}{2}\dot{e}^T D(q)\dot{e} + \frac{1}{2}e^T k_p e + \frac{1}{2}\text{trace}(\tilde{\Theta}^T \Gamma^{-1}\tilde{\Theta})$ be a candidate Lyapunov function, and we note that $V(e,\dot{e},\tilde{\Theta}) > 0$, since $D(q) > 0$, $k_p > 0$ and $\Gamma > 0$. Then, taking the time derivative of $V(\cdot)$ along the trajectory of (17) to obtain

$$\dot{V} = \dot{e}^T D(q)\ddot{e} + \frac{1}{2}\dot{e}^T \dot{D}(q)\dot{e} + e^T k_p \dot{e} + \text{trace}(\tilde{\Theta}^T \Gamma^{-1}\dot{\tilde{\Theta}}).$$

Now, substituting (17) into above and enforcing the Property II presented earlier, we obtain

$$\dot{V}(e,\dot{e},\tilde{\Theta}) = -\dot{e}^T k_d \dot{e} + \dot{e}^T \tilde{\Theta}^T \Pi + \text{trace}(\tilde{\Theta}^T \Gamma^{-1}\dot{\tilde{\Theta}}).$$

Note that given two matrices A and B of compatible dimensions, we have the following identity:

$$\text{trace}(AB) = \text{trace}(BA).$$

Hence, $\dot{e}^T \tilde{\Theta}^T \Pi = \text{trace}(\tilde{\Theta}^T \Pi \dot{e}^T)$. Substituting this into above yields

$$\dot{V}(e,\dot{e},\tilde{\Theta}) = -\dot{e}^T k_d \dot{e} + \text{trace}[\tilde{\Theta}^T(\Pi \dot{e}^T + \Gamma^{-1}\dot{\tilde{\Theta}})],$$

and by utilizing the parameter adaption law given in (18), we obtain

$$\dot{V}(e,\dot{e},\tilde{\Theta}) = -\dot{e}^T k_d \dot{e} \leq 0,$$

that is $\dot{V}(\cdot)$ is bounded for all $(e,\dot{e},\tilde{\Theta})$. To show that $\dot{V}(\cdot) \to 0$ as $t \to \infty$, we must prove that $\dot{V}$ is uniformly continuous, which can be determined by first examining if $\ddot{V}(\cdot)$ is bounded. Now, we take the time derivative of $\dot{V}(\cdot)$ along the trajectory of (17) to obtain

$$\ddot{V}(e,\dot{e},\tilde{\Theta}) = -2\dot{e}^T k_d \ddot{e},$$

and by examining the terms in (17) we can readily deduce that $\ddot{e}$ is bounded, hence $\ddot{V}(\cdot)$ is bounded. Finally, it follows from the Barbalat's lemma[6] that $\dot{V}(\cdot) \to 0$, and hence $e(t) \to 0$ as $t \to \infty$. We should also note that the estimation error $\tilde{\Theta}$ is only bounded. This concludes the proof. QED

American Institute of Aeronautics and Astronautics

V. Control of Flexible Space Structures

Recall the flexible structure dynamics described in (11). We assume there are m number of control actuators instrumented along the span of structure, as illustrated in Fig. 4. Then, with the implementation of active controls, (11) can be augmented as

$$M_s \ddot{p}(t) + C_s \dot{p}(t) + K_s p(t) = B(x_v) f_z(\theta_1, \theta_2) + \sum_{i=1}^{m} B(x_i) u_i(t), \tag{19}$$

where u_i denotes the ith control input and $B(x_i)$ its location given by

$$B(x_i) = \begin{bmatrix} \Phi_1(x_i) \\ \Phi_2(x_i) \\ \vdots \\ \Phi_n(x_i) \end{bmatrix}.$$

It should be noted that, while the placement of control inputs are considered fixed, the coupling effect $f_z(\theta_1, \theta_2)$ induced by a walking robot is changing as indicated in the matrix $B(x_v)$, where x_v progresses forward. For the purpose of control design, we treat $B(x_v) f_z(\theta_1, \theta_2)$ as a vector of disturbance input $Dw(t)$ to the beam structure, where $w(t)$ is considered as a weighted $\mathscr{L}_2$ disturbance input with weighting matrix $W^T = W > 0$.[7] In addition, we assume that both the deflection and deflection rate are available for measurement and co-located with the actuators; that is, there are m position sensors and m velocity sensors placed at $B(x_i)$. We are keenly aware the complication involved in data processing and conversion required from measured strain gauge/gyro data to actually be used for feedback design. That would be a subject for future study.

If $z_p(t)$ denotes the measured output, then

$$z_p(t) = \underbrace{\begin{bmatrix} B_x^T & B_x^T \end{bmatrix}}_{M_p} \begin{bmatrix} p(t) \\ \dot{p}(t) \end{bmatrix}, \text{ where } B_x = \begin{bmatrix} B(x_1) & B(x_2) & \cdots & B(x_n) \end{bmatrix}. \tag{20}$$

It should be noted that B_x has full column rank, and z_p and u have the same dimensions.
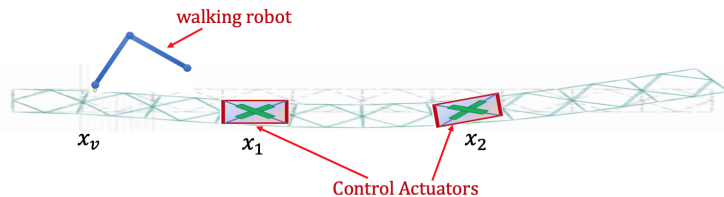

Figure 4. Placement of actuators in the structure.

V.A. A canonical system representation

Let $x_p = [p^T \ \dot{p}^T]^T$ be a vector of states, then the state-space representation for (19) can be written as

$$\Sigma_o : \begin{cases} \dot{x}_p(t) = A_p x_p(t) + B_p u(t) + D_p w(t) \\ z_p(t) = M_p x_p(t) \\ y_p(t) = C_p x_p(t) \end{cases} \tag{21}$$

where $u = [u_1 \ u_2 \ \cdots u_m]^T$ denotes the control input, y_p the controlled or performance output, and

$$A_p = \begin{bmatrix} 0 & I \\ -M_s^{-1} K_s & -M_s^{-1} C_s \end{bmatrix}, B_p = \begin{bmatrix} 0 \\ M_s^{-1} B_x \end{bmatrix}, D_p = \begin{bmatrix} 0 \\ M_s^{-1} D \end{bmatrix}, C_p = M_p.$$

In this study, we are interested in assessing the output responses at those sensor locations, hence we choose $y_p = z_p$. Furthermore, it is important to note that the high gain matrix $M_p B_p$ is nonsingular. We introduce the following definition of system zeros for Σ_o.

Definition 1: A complex number s_0 is a zero of the system Σ_o, if and only if the matrix

$$\Lambda(s_0) = \begin{bmatrix} s_0 I - A_p & B_p \\ M_p & 0 \end{bmatrix} \tag{22}$$

is singular.

The next lemma presents a coordinate transformation for Σ_o that results in a special structure. This representation plays a key role in our subsequent derivation for the direct output feedback controllers.

Lemma 1. *There exists a nonsingular coordinate transformation matrix T such that, with $\eta(t) = T p(t)$, the system Σ_o can be equivalently described by*

$$\hat{\Sigma}_o : \begin{cases} \dot{\eta}(t) = \hat{A}_p \eta(t) + \hat{B}_p u(t) + \hat{D}_p w(t) \\ z_p(t) = \hat{M}_p \eta(t) \end{cases} \tag{23}$$

where

$$\hat{A}_p = T A_p T^{-1} = \begin{bmatrix} A_{11} & A_{12} \\ A_{12} & A_{22} \end{bmatrix}, \hat{B}_p = T B_p = \begin{bmatrix} 0 \\ I_m \end{bmatrix}, \hat{D}_p = T D_p = \begin{bmatrix} D_1 \\ D_2 \end{bmatrix}, \hat{M}_p = M_p T^{-1} = \begin{bmatrix} 0 & (M_p B_p) \end{bmatrix}. \tag{24}$$

Moreover, the eigenvalues of A_{11} coincide with the system zeros of Σ_o.

Proof: First, we perform the singular value decomposition for B_p to obtain

$$B_p = \begin{bmatrix} U_1 & U_2 \end{bmatrix} \begin{bmatrix} 0 \\ \Sigma \end{bmatrix} V_1^T,$$

which implies that $U_1^T B_p = 0$. Now, we choose

$$T = \begin{bmatrix} U_1^T \\ (M_p B_p)^{-1} M_p \end{bmatrix},$$

then T^{-1} would have the structure of $[S \ \ B_p]$. Let $\eta(t) = T p(t)$, then Σ_o can be described in $\eta-$coordinate as shown in $\hat{\Sigma}_o$. To prove that the eigenvalues of A_{11} are the system zeros, we first note that the system zeros are invariant under coordinate transformation. Hence, after substituting the partitions of $(\hat{A}_p, \hat{B}_p, \hat{M}_p)$ into (22) yields

$$\hat{\Lambda}(s_0) = \begin{bmatrix} s_0 I - A_{11} & -A_{12} & 0 \\ -A_{21} & s_0 I - A_{22} & I_m \\ 0 & (M_p B_p) & 0 \end{bmatrix}.$$

Utilizing the fact that, given any two matrices X and Y with X invertible, then $rank(XY) = rank(Y)$. We obtain

$$\hat{\Lambda}(s_0) = \begin{bmatrix} I & 0 & -A_{12}(M_p B_p)^{-1} \\ 0 & I_m & (s_0 I - A_{22})(M_p B_p)^{-1} \\ 0 & 0 & I_m \end{bmatrix} \begin{bmatrix} s_0 I - A_{11} & 0 & 0 \\ -A_{21} & I_m & 0 \\ 0 & 0 & (M_p B_p) \end{bmatrix} \begin{bmatrix} I & 0 & 0 \\ 0 & 0 & I_m \\ 0 & I_m & 0 \end{bmatrix}.$$

It can be readily shown that the matrix $\hat{\Lambda}(s_0)$ becomes singular, if and only if the matrix

$$\begin{bmatrix} s_0 I - A_{11} & 0 & 0 \\ -A_{21} & I_m & 0 \\ 0 & 0 & (M_p B_p) \end{bmatrix} \tag{25}$$

is singular, and this is equivalent to that the matrix $s_0 I - A_{11}$ is singular. This proves that the system zeros of Σ_o are the eigenvalues of A_{11}. QED

For a structure model given in (19), we can further prove that the system Σ_o is strictly minimum phase, that is, all its system zeros lie in the open left half of the complex plane. Therefore, the matrix A_{11} is strictly Hurwitz. We shall take advantage of this fact in the subsequent output control design process. One of the key features of a minimum phase system is that, when needed, the implementation of large output control gain is possible, in order to achieve the desired performance.

V.B.   Output covariance constraint problem

We consider the following system,

$$\begin{cases} \dot{x}(t) = Ax(t) + Dw(t) \\ y(t) = Cx(t) \end{cases} \tag{26}$$

where (C, A, D) are matrices of compatible dimensions and $w(t)$ a weighted $\mathscr{L}_2$ disturbance input with weighting matrix $W > 0$. It is given that, if A is Hurwitz, then the output covariance for (26) is given by[8]

$$Y = CXC^T, \tag{27}$$

where X is the controllability Gramian matrix satisfying the following Lyapunov equation

$$XA^T + AX + DWD^T = 0. \tag{28}$$

Now, if $\bar{Y}$ is the desired output covariance for $y(t)$, then the output covariance constraint problem[7] for (26) is said to be solved, if

$$Y \leq \bar{Y}. \tag{29}$$

In this paper, we focus on characterizing the output covariance optimization problem by utilizing the linear matrix inequalities (LMIs). Let $\varepsilon > 0$ be given, and we consider the following parameterized Lyapunov equation,

$$\bar{X}A^T + A\bar{X} + DWD^T + \varepsilon I = 0, \tag{30}$$

where $\bar{X}$ is a unique positive definite solution. It follows from the monotonicity of the Lyapunov solutions that $\bar{X} > X$. Therefore, (27) and (29) can be modified as

$$C\bar{X}C^T < \bar{Y}, \tag{31}$$

and (30) can be rewritten as

$$\bar{X}A^T + A\bar{X} + DWD^T < 0. \tag{32}$$

Finally, by applying the Schur complement argument to (32),[9] we obtain the following LMI expression,

$$\begin{bmatrix} \bar{X}A^T + A\bar{X} & DQ \\ QD^T & -I \end{bmatrix} < 0, \tag{33}$$

where $Q = W^{\frac{1}{2}}$. Note that (33) is an affine function in both $\bar{X}$ and Q, and hence can be effectively solved by using, for instance, interior-point methods from convex optimization.[10] In summary, the output covariance constraint problem can be characterized in the next lemma, whose proof follows readily from the arguments given above.

Lemma 2. *Consider (26) and let $\bar{Y} > 0$ be the desired output covariance. Then, the output covariance constraint problem is solvable, if there exists $\bar{X} > 0$ satisfying*

  (i) *(33) is feasible;*

 (ii) $C\bar{X}C^T \leq \bar{Y}$.

V.C.   LMI-based optimal static output feedback control

In this paper, we propose to solve the output covariance constraint problem for Σ_o by utilizing the static output feedback controller of the form,

$$u(t) = -Kz(t), \tag{34}$$

where K is the control gain to be determined. Recall that A_{11} is strictly Hurwitz, then let

$$\bar{\alpha} = -\max\{\text{Re}(s_0) : s_0 \text{ is an eigenvalue of } A_{11}\} > 0. \tag{35}$$

Suppose we choose $\alpha > 0$, with $\alpha < \bar{\alpha}$, to be a desired rate of convergence for the feedback-controlled system. Since the matrix $A_{11} + \alpha I$ is strictly Hurwitz for all $\alpha < \bar{\alpha}$, thus for any given $Q_{11} > 0$, the following Lyapunov inequality equation,

$$X_{11}(A_{11} + \alpha I)^T + (A_{11} + \alpha I)X_{11} + D_1WD_1^T + Q_{11} < 0, \tag{36}$$

admits a positive definite symmetric solution X_{11}.

Lemma 3. *Consider the system Σ_o. Suppose $\alpha > 0$ with $\alpha < \bar{\alpha}$ is given. If there exist a positive definite symmetric matrix X, a nonsingular matrix K, and a positive scalar γ satisfying*

(i) $X(A_p + \alpha I)^T + (A_p + \alpha I)X - \gamma B_p B_p^T + D_p W D_p^T < 0$;

(ii) $\gamma K^{-1} B_p^T = M_p X$.

Then, the static output feedback controller given in (34) asymptotically stabilizes Σ_o with convergent rate α.

Proof: Let $P = X^{-1} > 0$ and pre- and post-multiply (i) by P, we obtain

$$(A_p + \alpha I)^T P + P(A_p + \alpha I) - \gamma P B_p B_p^T P + P D_p W D_p^T P < 0. \tag{37}$$

Now, substituting (ii) into (37), and add and subtract the term $\gamma P B_p B_p^T P$, then (37) can be rewritten as

$$(A_p - B_p K M_p + \alpha I)^T P + P(A_p - B_p K M_p + \alpha I) + \underbrace{\gamma P B_p B_p^T P + P D_p W D_p^T P}_{\geq 0} < 0.$$

It then follows readily from the Lyapunov stability theory that the matrix $(A_p - B_p K M_p + \alpha I)$ is strictly Hurwitz. In other words, with the output feedback controller (34), the real parts of the eigenvalues of the closed-loop system matrix, $A_p - B_p K M_p$, are strictly less than $-\alpha$. QED

In Lemma 3, the sufficient conditions for the existence of direct output feedback control are given. Now, it is left to construct such X, K, and γ that satisfy Conditions (i) and (ii), and also solve the output covariance constraint problem.

First, partition X according to the partition of $\hat{A}_p$ as follows,

$$X = \begin{bmatrix} X_{11} & X_{12} \\ X_{12}^T & X_{22} \end{bmatrix},$$

where $X_{11} > 0$ solves (36) and the rest are to be determined. It follows from the matrix partitions given in (24) that Condition (ii) becomes

$$\gamma[0 \quad K^{-1}] = [(M_p B_p)X_{12}^T \quad (M_p B_p)X_{22}],$$

which implies that $X_{12} = 0$, and the control gain matrix K is then given by

$$K = \gamma(M_p B_p X_{22})^{-1}, \tag{38}$$

where $\gamma > 0$ and $X_{22} > 0$ are yet to be determined. Consider the inequality in Condition (i), and we substitute the system matrices given in (24) to obtain the LMI as follows,

$$\mathscr{A} = \begin{bmatrix} X_{11}(A_{11} + \alpha I)^T + (A_{11} + \alpha I)X_{11} + D_1 W D_1^T & X_{11}A_{21}^T + A_{12}X_{22} + D_1 W D_2^T \\ X_{22}A_{12}^T + A_{21}X_{11} + D_2 W D_1^T & \mathscr{Y}_{22} \end{bmatrix} < 0 \tag{39}$$

where $\mathscr{Y}_{22} = X_{22}(A_{22} + \alpha I)^T + (A_{22} + \alpha I)X_{22} + D_2 W D_2^T - \gamma I$. Then, it follows from (36) that $\mathscr{A}(1,1) = -Q_{11} < 0$, hence by utilizing the Schur complement argument, $\mathscr{A} < 0$ if and only if there exist $\gamma > 0$ and $X_{22} > 0$, such that

$$\mathscr{Y}_{22} + (X_{22}A_{12}^T + A_{21}X_{11} + D_2 W D_1^T)Q_{11}^{-1}(X_{11}A_{21}^T + A_{12}X_{22} + D_1 W D_2^T) < 0. \tag{40}$$

In summary, we have the following theorem that presents a solution to the optimal output covariance constraint problem using a static output feedback controller.

Theorem 1. *Consider the system Σ_o described in (21). Given $\alpha > 0$ with $\alpha < \bar{\alpha}$, the optimal output covariance control problem, at a rate of convergence α, is solvable with the static output feedback controller given in (34), if there exist a positive definite symmetric matrix X and $\gamma > 0$ that minimize the performance cost*

$$\min_{\gamma,X} trace \left\{ C_p X C_p^T \right\}, \tag{41}$$

subject to

$$X(A_p + \alpha I)^T + (A_p + \alpha I)X - \gamma B_p B_p^T + D_p W D_p^T < 0. \tag{42}$$

Furthermore, if there exists a feasible solution to the above LMI, then the static output feedback gain K is given by

$$K = \gamma(M_p B_p)^{-1}. \tag{43}$$

Proof: The proof follows from Lemmas 2 and 3, and the arguments given above. QED

American Institute of Aeronautics and Astronautics

VI. Numerical Study

We consider a robot walking on a 1-km long flexible structure. The structure is built by assembling a collection of voxel substructures shown in Fig. 5. The pitch length of a voxel substructure is 0.3048 m and each voxel (with necessary connection parts) weights 0.374 kg. The modulus of structure E is obtained from the stress analysis performed for a structure dimension of 10-voxel by 10-voxel by 10-voxel (i.e. 1000 voxels), and it is determined that $E \approx 24.5$ Mpa. As a result, the cross-sectional area of this 1-km structure is chosen to be 10-voxel by 10-voxel, therefore in total there are 328,100 voxels, and the mass per unit length ρA is 122 kg/m and the area moment of inertia I is 7.1925 m^4.

A two-legged walking robot is illustrated as in Fig. 2. For this study, the leg-1 parameters are chosen to be: $M_1 = 0.414$ kg, $l_1 = 0.1855$ m, $L_1 = 0.4$ m, $I_1 = 9.0269 \times 10^{-3}$ kg-m^2, and the leg-2 parameters: $M_2 = 1.636$ kg, $l_2 = 0.4$ m, $L_2 = 0.5$ m, $I_2 = 4.963 \times 10^{-2}$ kg-m^2. In this case, we are simulating a walking scenario where leg-2 is moving forward while carrying a voxel, hence leg-2 would have higher mass and inertia. Subsequently, leg-1 will move forward and land right behind leg-2. This will complete a walking cycle.
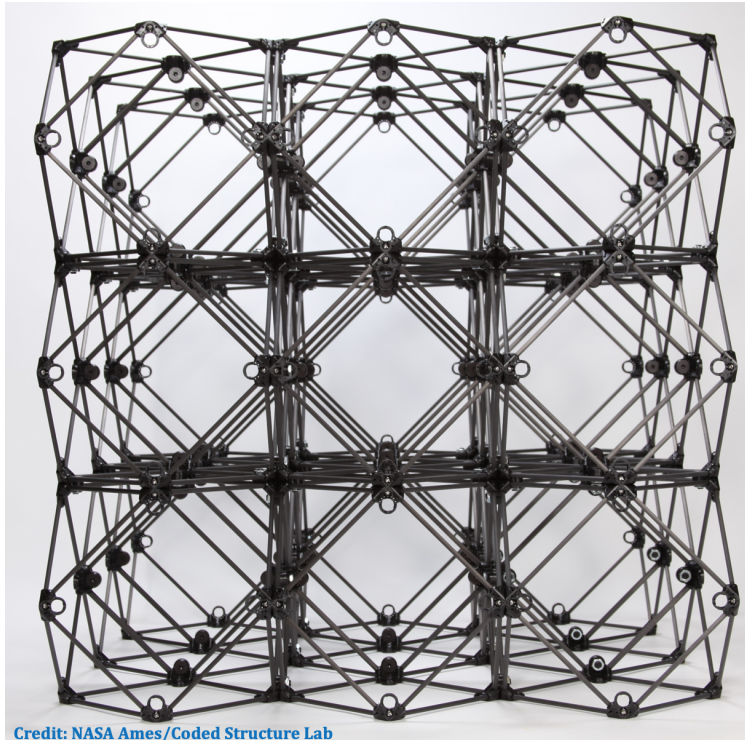
Figure 5. A volumetric pixel (or voxel) substructure: $3 \times 3 \times 3$ (total 27 voxels).

VI.A. Trajectory tracking

Figure 6 shows a robot walking on a flexible structure, in which θ_1 and θ_2 are depicted at discrete instant of time. A third order polynomial function is used to approximate θ_1 and θ_2 positions; as shown in Fig. 7, and these are then used to generate a desired robot trajectory $q_d(t)$, for $t_0 \leq t \leq t_4$, as follows,

$$q_d(t) = \begin{bmatrix} \theta_1^d(t) \\ \theta_2^d(t) \end{bmatrix}, \ \theta_1^d(t) = a_0 + a_1 t + a_2 t^2 + a_3 t^3 \text{ and } \theta_2^d(t) = b_0 + b_1 t + b_2 t^2 + b_3 t^3, \tag{44}$$

where $[a_0, a_1, a_2, a_3] = [69.7000, 3.4917, -0.2250, 0.0031]$ and $[b_0, b_1, b_2, b_3] = [19.6143, 1.7988, -0.0039, -0.0007]$. Note that Fig. 6 shows the scenario where leg-2 moves forward, however a similar trajectory can be generated for leg-1 moving forward.

The coupling force inserted by robot (leg-1) during leg-2 moving forward can be computed from (2c), except we neglect the gravity term and the structure reaction term. This force can then be considered as an external disturbance force $w(t)$ to the underline structure.
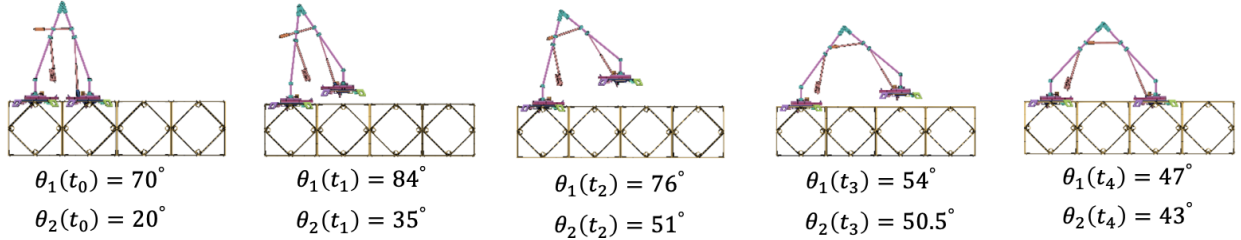
| $\theta_1(t_0) = 70°$ | $\theta_1(t_1) = 84°$ | $\theta_1(t_2) = 76°$ | $\theta_1(t_3) = 54°$ | $\theta_1(t_4) = 47°$ |
| $\theta_2(t_0) = 20°$ | $\theta_2(t_1) = 35°$ | $\theta_2(t_2) = 51°$ | $\theta_2(t_3) = 50.5°$ | $\theta_2(t_4) = 43°$ |

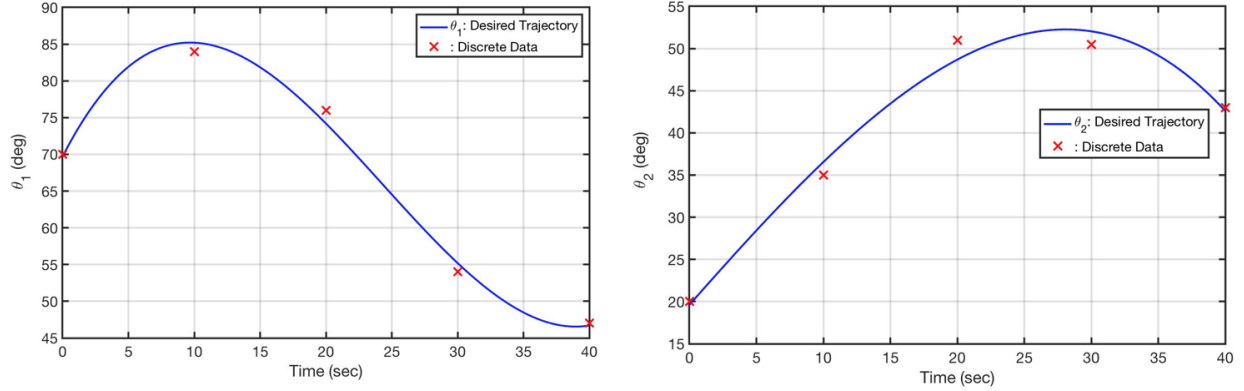**Figure 6. Robot walking on a flexible structure.**

Figure 7. Desired trajectory for θ_1 and θ_2.

VI.B.   Simulation results

We consider 10 flexible structure modes in bending and their undamped natural frequencies Ω are given by

$$\Omega = [0.0045, 0.0148, 0.0314, 0.0535, 0.0820, 0.1160, 0.1562, 0.2008, 0.2530, 0.3082]\,\text{rad/sec}.$$

In addition, as illustrated in Section III.B, we insert the structure damping ratio of 5% into the structure. As shown in Fig. 8, there are 5 active actuators instrumented within the structure, and hence 5 position and 5 rate sensors, where $[x_1, x_2, x_3, x_4, x_5] = [100, 300, 500, 700, 900]$m. We assume the disturbance $w(t)$ has the intensity $W = 0.0156$, which is computed by following the walking scenario shown in Figs. 6 and 7. It was determined from Lemma 1 that $\bar{\alpha} = 0.009$, hence we choose α to be 0.008. The LMI constraint in Theorem 1 is implemented and solved in MATLAB environment by utilizing SeDuMi as optimization solver and Yalmip as LMI parser, subsequently a static output feedback controller is obtained as function of γ.

The impulse responses are assessed in this study, where an impulse is applied at point x_3 in Fig. 8. Figures 9-10 show the time history of the deflection and velocity at points x_1 and x_3, respectively, for the open-loop and closed-loop (with the static output feedback at $\gamma = 100$). These simulation results demonstrate that the proposed direct output feedback controller can effectively suppress the excessive structure vibration. It is also worth mentioning that the added control effort only amounts to about 1% and 0.1% addition to the structure damping and stiffness, respectively. Figure 11 shows the eigenvalue map of the closed-loop system as γ increases. It can be clearly seen that, as $\gamma \approx \infty$, some of the closed-loop poles approach some finite values, while others move to infinity. These finite poles precisely coincide with those (finite) system zeros, and their locations ultimately determine the closed-loop system performance when very large control gain γ is applied. Therefore, in actual implementation a practically allowable control effort will need to be calibrated and incorporated as an additional LMI constraint in Theorem 1.

VII.   Summary

This paper presented a numerically tractable problem formulation for modeling and control of coupled robot-structure dynamics. For controlling a walking robot on a flexible structure, we proposed a robotic controller that
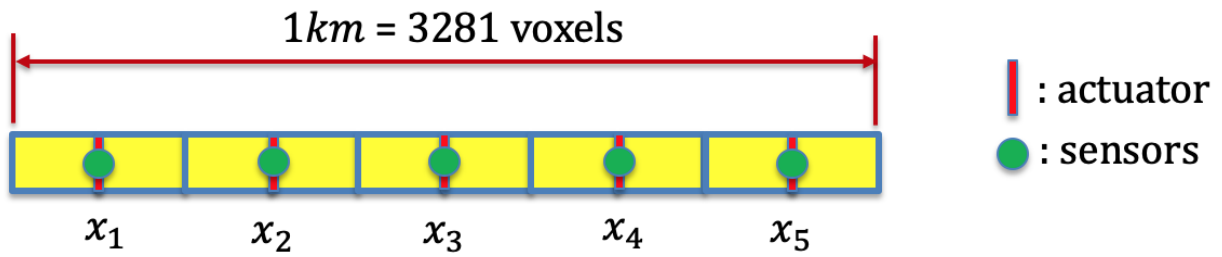
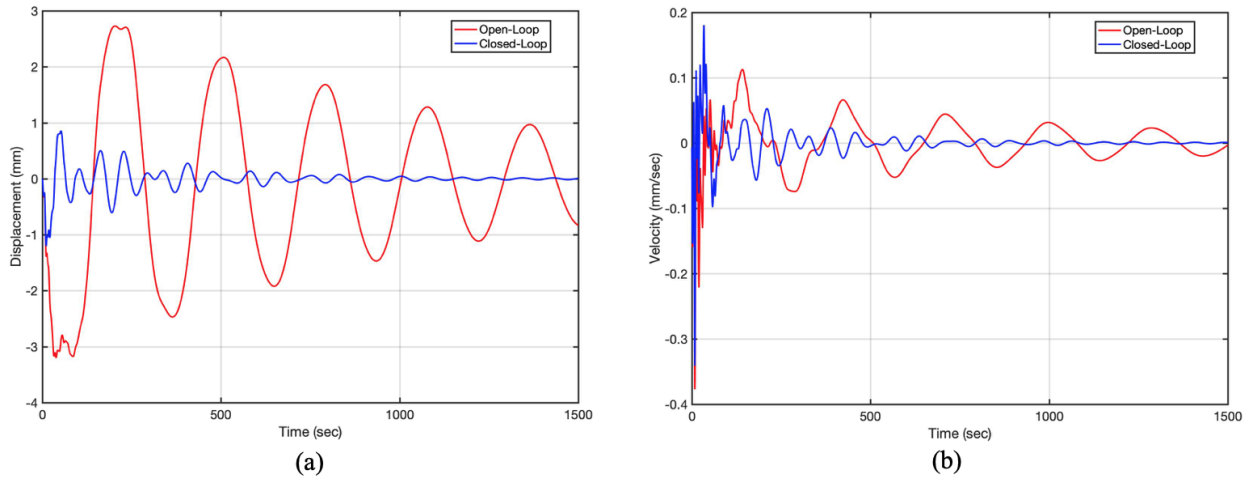**Figure 8. Distributed actuators and sensors in the structure.**

(a)

(b)

Figure 9. Impulse response comparisons at point x_1: (a) displacement; (b) velocity.
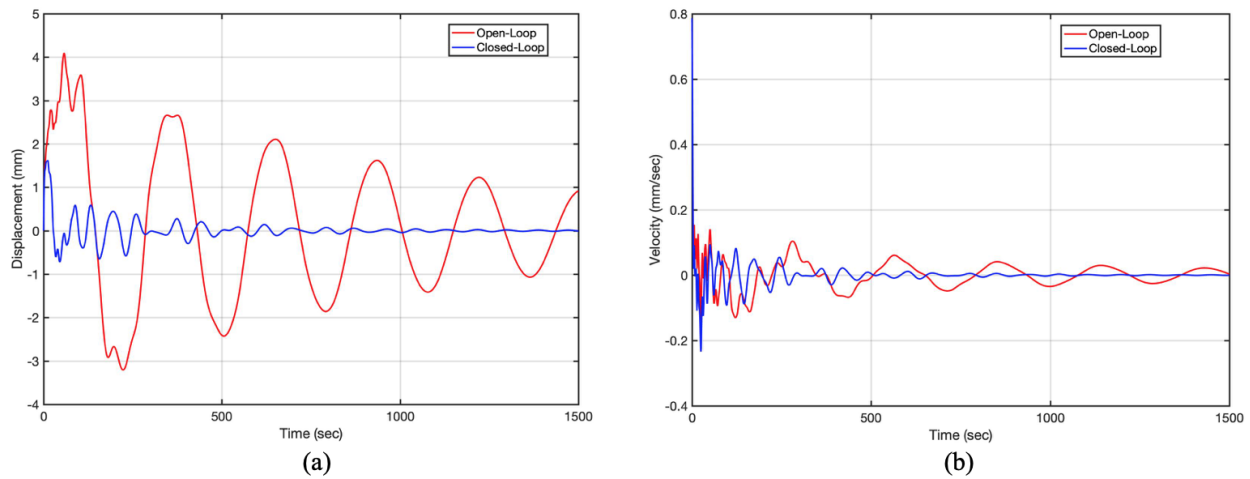

(a)

(b)

Figure 10. Impulse response comparisons at point x_3: (a) displacement; (b) velocity.

consists of a conventional full state feedback motion controller and an adaptive controller. The adaptive controller is designed for accommodating coupling dynamics induced from the flexible structure while robot moving forward. The Euler-Bernoulli beam approximation was utilized to model the "free-free" flexible space structure. A finite set of co-located sensors and actuators were distributed along the structure, and a direct static output feedback controller
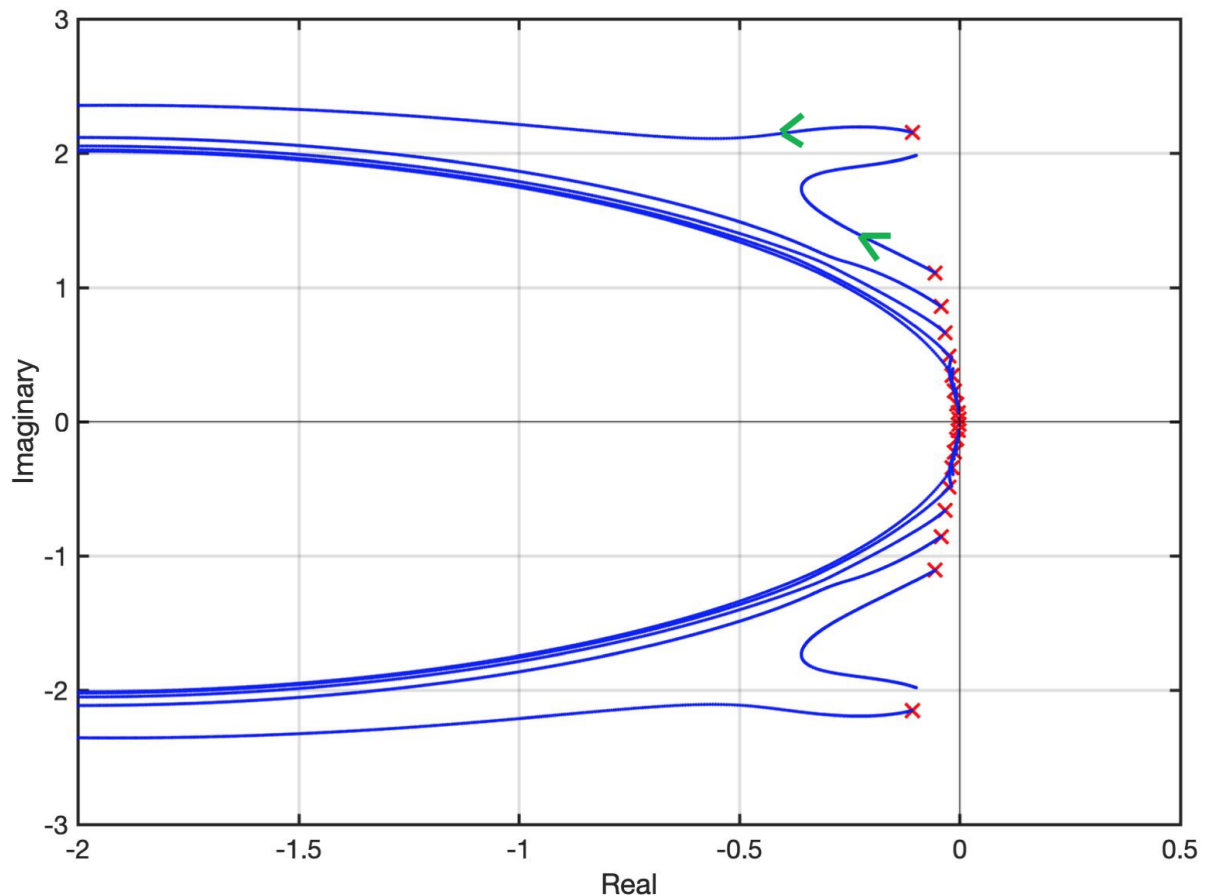
American Institute of Aeronautics and Astronautics

Figure 11. Root-locus as γ increases.

was proposed by utilizing the LMI characterization for optimal output covariance constraint control problem, in which the presence of walking robots were considered as bounded disturbance inputs to the structure. The simulation results showed the efficacy of the proposed framework.

In this study, we have only considered the structure dynamics in bending, the torsional and bending-torsion coupling are critical structure behaviors that can not be ignored. In addition, a practical number of sensors/actuators and their placement on the structure are another important subject of research. These will be included in the future study.

Acknowledgments

References

[1]Cramer, C., Cellucci, D., Formoso, O., Gregg, C., Jenett, B., Kim, J., Lendraitis, M., Swei, S., Trinh, G., Trinh, K., Cheung, K., "Elastic Shape Morphing of Ultralight Structures by Programmable Assembly," *Smart Mater. Struct.*, 28, 2019

[2]Jenett, B., Gregg, C., Cheung, K., "Feasibility Study of a Kilometer Solar Array Using Discrete Lattice Materials and Distributed Mobile Robots," *70th International Astronautical Congress*, Washington D.C., October 2019.

[3]Balas, M.J., "Trends in Large Space Structure Control Theory: Fondest Hopes, Wildest Dreams," *IEEE Transaction on Automatic Control*, vol. 27, no. 3, 1982.

[4]Jenett, B., Cheung, K., "BILL-E: Robotic Platform for Locomotion and Manipulation of Lightweight Space Structures," *AIAA SciTech*

Forum, Grapevine, TX, January 2017.

[5]Spong, M., Vidyasagar, M., *Robot Dynamics and Control*, John Wiley & Sons, 1989

[6]Slotine, J., Li, W., *Applied Nonlinear Control*, Prentice-Hall, Inc., 1991

[7]White, A., Zhu, G., Choi, J., "'A Linear Matrix Inequality Solution to the Output Covariance Constraint Control Problem,"' *ASME Dynamic Systems and Control Conf.*, Fort Lauderdale, FL, 2012.

[8]Skelton, R. E., *Dynamics System Control*, Wiley, New York, 1988.

[9]Kailath, T., *Linear Systems*, Prentice-Hall, Inc., 1980.

[10]Nesterov, Y., and Nemirovskii, A., *Interior-Point Polynomial Algorithms in Convex Programming*, *Studies in Applied and Numerical Mathematics*, SIAM, Philadelphia, 1994.

American Institute of Aeronautics and Astronautics